Rhizosphere-enhanced biosurfactant action on slowly desorbing PAHs in contaminated soil

Rosa Posada-Baquero,[†] Sara Nienke Jimenez-Volkerink,[‡] José Luis García,[†] Joaquim Vila,[‡] Manuel Cantos,[†] Magdalena Grifoll,[‡] and Jose Julio Ortega-Calvo*,[†]

[†]Instituto de Recursos Naturales y Agrobiología de Sevilla (IRNAS-CSIC), Avenida Reina Mercedes, 10, Seville 41012, Spain

[‡]Departament de Genètica, Microbiologia i Estadística, Facultat de Biologia, Universitat de Barcelona, Diagonal 643, Barcelona 08028, Spain

Running title: Biosurfactants and the rhizosphere enhance pollutant biodegradation

Keywords: Bioavailability; Biodegradation; Bacteria; Polycyclic aromatic hydrocarbons; Bioremediation; Sunflower

ABSTRACT: We studied how sunflower plants affect rhamnolipid biosurfactant mobilization of slowly desorbing fractions of polycyclic aromatic hydrocarbons (PAHs) in soil from a creosote-contaminated site. Desorption kinetics of 13 individual PAHs revealed that the soil contained initially up to 50% slowly desorbing fractions. A rhamnolipid biosurfactant was applied to the soil at the completion of the sunflower cycle (75 days in greenhouse conditions). After this period, the PAHs that remained in the soil were mainly present in a slowly desorbing form as a result of the efficient biodegradation of fast-desorbing PAHs by native microbial populations. The rhamnolipid enhanced the bioavailable fraction of the remaining PAHs by up to 30%, as evidenced by a standardized desorption extraction with Tenax, but the enhancement occurred with only planted soils. The enhanced bioavailability did not decrease residual PAH concentrations under greenhouse conditions, possibly due to ecophysiological limitations in the biodegradation process that were independent of the bioavailability. However, biodegradation was enhanced during slurry treatment of greenhouse planted soils that received the biosurfactant. The addition of rhamnolipids caused a dramatic shift in the soil bacterial community structure, which was magnified in the presence of sunflower plants. The stimulated groups were identified as fast-growing and catabolically versatile bacteria. This new rhizosphere microbial biomass possibly interacted with the biosurfactant to facilitate intra-aggregate diffusion of PAHs, thus enhancing the kinetics of slow desorption. Our results show that the usually limited biosurfactant efficiency with contaminated field soils can be significantly enhanced by integrating the sunflower ontogenetic cycle into the bioremediation design.

GRAPHICAL ABSTRACT

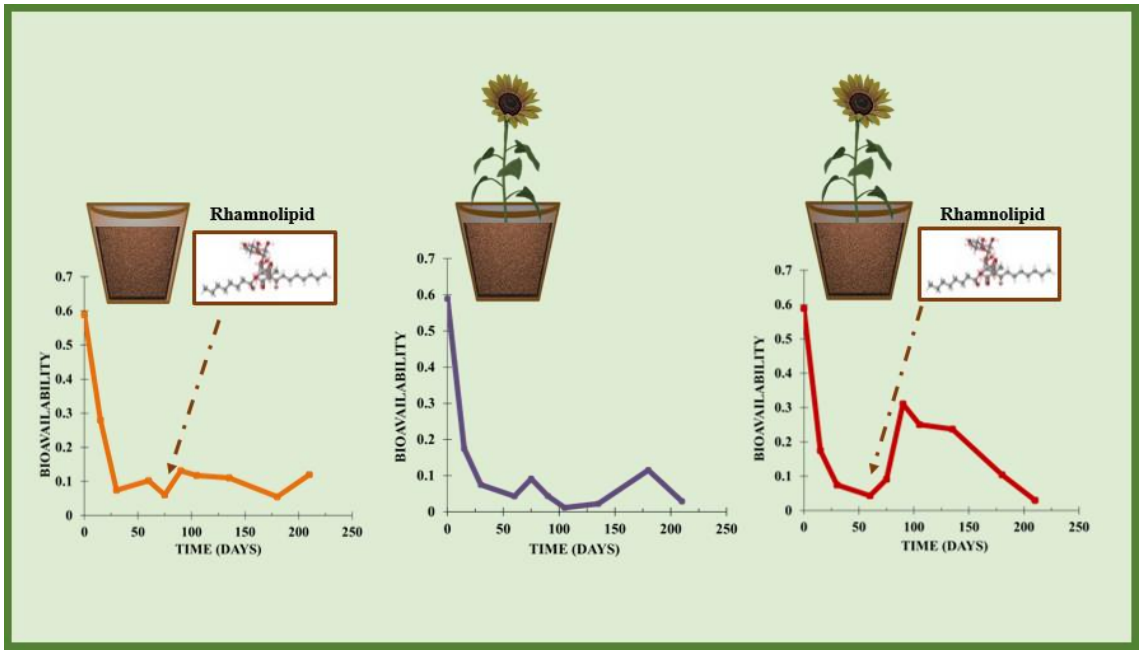

INTRODUCTION

The management of soil pollution through biologically based remediation is challenging when the residual concentrations of pollutants after treatment are unacceptable, especially for hydrophobic organic chemicals such as polycyclic aromatic hydrocarbons (PAHs). The well-established biphasic desorption behavior of these compounds in soil allows us to discriminate risks at remediation endpoints because fast-desorbing chemicals are those causing the highest toxicity and they are preferentially removed (Ortega-Calvo et al., 2015). However, with half-lives on the order of months or years, slowly desorbing PAHs, remaining in polluted soils after bioremediation, can also be degraded slowly or they may still be absorbed by biota and cause toxic effects. Therefore, it is imperative to understand the mechanisms of slow release of the residual pollutant fractions, and find benign strategies to improve their biodegradation. Potential strategies include the use of specific microorganisms, plants and (bio)surfactants, which can act as bioavailability-promoting agents (Ortega-Calvo et al., 2013). When bioremediation scenarios include slowly desorbing PAHs, the rhamnolipid biosurfactant constitutes one of the most valid solutions. Its nontoxic, biodegradable and environmentally benign nature and its possibilities for large-scale production at competitive costs make this biosurfactant a standard for environmental applications (Posada-Baquero et al., 2019a). However, the biosurfactant efficiency with aged, slowly desorbing PAHs decreases compared with the efficiency with unaged samples as a result of the limitations imposed by the intra-aggregate diffusion of the chemicals (Congiu and Ortega-Calvo, 2014). Further knowledge is needed to enhance the biosurfactant efficiency under the unfavorable conditions operating incontaminated field soils, where pollutants have been aged for years.

Sunflower (*Helianthus annuus*, L.) combines food and fuel value together with a proven phytoremediation potential for soils polluted by PAHs (Sivaram et al., 2018, Tejeda-Agredano et al., 2013). The sunflower ontogenetic cycle has a variable duration according to the variety used and the specific conditions of culture location, but it usually lasts from 3 to 5 months (Rondanini et al., 2007)(Cheng et al., 2014), which obviously should be considered in phytoremediation design. Its capacity to release organic compounds into soil by rhizodeposition is well known (Shahbaz et al., 2018) and the basis for the removal of pollutants through biodegradation by rhizosphere microorganisms (Tejeda-Agredano et al., 2013). The rhizosphere effect of sunflower is also well known and often results in higher rates of SOM decomposition in soils planted with sunflower than in unplanted soils (Zhu et al., 2014). Despite these advancements, the exact contribution of decaying sunflower root materials to PAH biodegradation at late stages of phytoremediation is still unknown. This is especially relevant for the slowly desorbing PAHs remaining in the soil after the completion of the sunflower cycle. Previous studies have considered the combined action of plants (including sunflower) and rhamnolipids on PAH dissipation (Liduino et al., 2018, Liao et al., 2015, Liao et al., 2016). It may be because they have received no attention that the indications of their impacts on the slowly desorbing PAH fractions, in connection with bioavailability measurements, are still relatively scarce.

Recent developments in the bioavailability and regulation of organic chemicals led to the proposal of a simplified approach for risk assessment based on total and bioavailable concentrations. A robust and reproducible physicochemical method, such as desorption extraction with a strong adsorbent, can be used to determine the bioavailability of organic chemicals (Ortega-Calvo et al., 2015, ISO/TS16751, 2018). We recently evaluated the general applicability of standardized desorption extraction as

a tool to evaluate the performance of bioremediation through bioavailability assessments in a wide variety of PAH-contaminated soils (Posada-Baquero et al., 2019b). The present study was designed to evaluate whether the biosurfactant action on slowly desorbing PAHs, assessed through standardized desorption extraction, could be enhanced by a previous stage of sunflower plant growth, which was not part of previous investigations. This new sequence was aimed at slowly desorbing PAHs and at minimizing the possible negative effects of biosurfactants on plant physiology. Therefore, the biosurfactant was applied at the end of the sunflower cycle. The whole process was characterized thoroughly by the desorption kinetics of individual PAHs, the evolution of their total and bioavailable concentrations, and the composition of the soil microbial populations as determined by molecular methods. To the best of our knowledge, there are no other studies in the bioremediation field that combine such approaches to systematically investigate changes in the bioavailability of organic pollutants. The objectives of this study were 1) to characterize the desorption kinetics of native PAHs in the soil, determining the exact abundance of the slowly desorbing fractions, 2) to determine the effect of planting and biosurfactant addition on the evolution of bioavailable PAHs in parallel to the composition and activity of the soil microbial community, and 3) to propose, on the basis of these results, mechanisms for improving rhamnolipid action on slowly desorbing PAHs in contaminated soils.

MATERIALS AND METHODS

Chemicals. [4,5,9,10-^{14}C]-pyrene (58.8 mCi mmol^{-1}, radiochemical purity >98%) was purchased from Campro Scientific GmbH (Veenendaal, The Netherlands). Tenax (60-80 mesh, 177-250 µm) was supplied by Buchem BV (Netherlands).

Rhamnolipid. The rhamnolipid biosurfactant (R90, 90% pure) was supplied by AGAE Technologies (Oregon, USA). The critical micelle concentration (CMC) of this biosurfactant, measured with a TD1 Lauda ring tensiometer, was 31.6 mg L^{-1}, at which a surface tension of 32 dyn cm^{-1} was achieved. The total organic carbon concentration (TOC) of the rhamnolipid, measured with a Shimadzu TOC-V SCH analyzer, was 47%.

Soil. A creosote-polluted soil mixture was obtained by combining a heavily polluted soil (silty clay loam-calcaric fluvisol, total PAH concentration 13,977 ± 567 mg kg^{-1}) from a historical wood-treatment facility in southern Spain, a soil (Typic Xerochrepts) from the agricultural experimental station of the Instituto de Recrusos Naturales y Agrobiología de Sevilla (IRNAS), and sand (Aquarama). The mixture provided plants with a suitable soil texture for growth. The PAH-containing soil mixture was prepared as indicated in the Supporting Information (SI). The total concentration of PAHs in this creosote-polluted soil was 513 ± 84 mg kg^{-1} (sum of 13 PAHs as indicated in Table S1). The soil had 1.1% TOC, 42.5% coarse-grained sand, 9.5% fine-grained sand, 26.8% silt, and 21.2% clay. Other soil characteristics are provided in the SI.

Greenhouse experiment. *Experimental design.* The greenhouse experimental design consisted of 30 pots with 4 kg of soil each. There were four different treatments, soil without plants (5 pots), soil with rhamnolipid (5 pots), soil with sunflower plants (10 pots), and soil with both rhamnolipid and sunflower plants (10 pots). A high number of planted pots ensured a sufficient quantity of plants with a homogenous root system and minimized the impact of intensive soil sampling on plant development by allowing rotated sampling in different plots. Ten sunflower seeds were used per planted pot. As the seeds germinated, they were eliminated until only one was left per pot to ensure one plant per pot during the experiment. The experiment was carried out in a greenhouse at

23 ± 1 ºC with watering at 20% field capacity. The pots were placed randomly and displaced along the greenhouse every 7 days to minimize light or temperature interferences. Soil samples were collected from the different treatments every 15 days up to the fourth month and then approximately every 30 days until the end of the experiment (210 days). The procedures for obtaining and storing soil samples for PAH and microbial analyses are described elsewhere (Tejeda-Agredano et al., 2013). Throughout sunflower development, the percentage of seed germination, blooming evolution and stem length of plants were separately evaluated for each treatment.

The rhamnolipid was applied to the soil after 75 days of treatment dissolved in 150 mL per pot of a 0.5 M tris-acetate buffer solution (pH 7.2) to give a final concentration of 7 mg g^{-1} soil. This concentration was selected in accordance with the methods in other studies involving the use of rhamnolipid to enhance the biodegradation of PAHs in contaminated soils (Posada-Baquero et al., 2019a, Adrion et al., 2016). The biosurfactant addition contributed 0.34% to the soil TOC (the buffer contributed less than 0.01% of TOC).

Standardized desorption extraction. The method used to assess the bioavailability of PAHs was based on Tenax acting as an infinite sink in a soil suspension. This standard method considers that the fraction of total PAHs extracted with Tenax for 20 h (D_{20}) represents most of the rapid desorption fraction and that this can be used as a measure of bioavailability. A detailed description of this method can be found in the ISO standard (ISO/TS16751, 2018), and its general applicability in bioremediation was reported in a previous publication (Posada-Baquero et al., 2019b). Single-point Tenax extractions of greenhouse soil samples taken at day 135 were subject to a detailed analysis of the chemical composition of the aqueous phase, as indicated in the SI.

The method to study the desorption kinetics in soil samples taken at the start of greenhouse experiments was the same as that described above, but for every sampling time, the Tenax was replaced by new Tenax. The experimental period was extended to 1057 h. Desorption data were fitted to a first-order, two-compartment model (Bueno-Montes et al., 2011):

$$S_t/S_0 = F_{fast}\exp(-K_{fast}t) + F_{slow}\exp(-K_{slow}t) \quad (1)$$

In this equation, S_t and S_o (mg) are the soil-sorbed amounts of PAHs at time t (h) and at the start of the experiment, respectively. F_{fast} and F_{slow} are the fast- and slow-desorbing fractions, and K_{fast} and K_{slow} (h^{-1}) are the rate constants of fast and slow desorption, respectively. To calculate the values of the different constants and fractions (F_{fast}, F_{slow}, K_{fast}, and K_{slow}), exponential curve fitting was used.

PAH analysis. Triplicate soil samples (1 g) were mixed and ground with 1 g of anhydrous sodium sulfate and then extracted in a Soxhlet apparatus for 8 h with 100 mL of 1:1 (v/v) dichloromethane/acetone. Acetone was used instead of this organic solvent mixture to completely extract the PAHs from soil samples taken from rhamnolipid-treated soils in greenhouse and slurry experiments. An analysis of 13 PAHs (as listed in Table S1) was carried out by HPLC as previously described (Posada-Baquero and Ortega-Calvo, 2011). The concentrations of PAHs were expressed either individually as mg kg^{-1} or as a fraction (C/C_0, where C_0 is the initial concentration) of the sum of mineralizable PAHs (mPAHs, including fluorene, phenanthrene, anthracene, fluoranthene, and pyrene) and cometabolizable PAHs (cPAHs, including benzo(*a*)anthracene, crysene, benzo(*b*)fluoranthene, benzo(*k*)fluoranthene, benzo*(a*)pyrene, dibenzo(*ah*)anthracene, benzo(*ghi*)perylene, and indeno(1,2,3-*cd*)pyrene). This distinction was based on operational reasons and the current knowledge of bioremediation of PAH-polluted soils (Ortega-Calvo et al., 2013).

193 *Bacterial community analyses.* Total nucleic acids were coextracted from three
194 separate aliquots (0.25 g) of soil samples using the PowerMicrobiome® kit (MoBio,
195 USA) following the manufacturer's instructions. Extracts were split into two aliquots
196 for DNA and RNA analysis. Aliquots for RNA analysis were treated with DNase I, and
197 the absence of contaminant DNA was confirmed by PCR using universal 16S rRNA
198 primers (341F and 518R). RNA was reverse-transcribed to cDNA using the High
199 Capacity Reverse Transcription kit (Applied Biosystems, USA) with random hexamers.
200 Detailed procedures for high throughput amplicon sequencing of the V4 region of 16S
201 rRNA from triplicate DNA and cDNA samples at selected time points, real-time PCR
202 (qPCR) analyses and statistical treatments are provided in the SI. Raw sequencing data
203 were submitted to the NCBI SRA repository under bioproject ID PRJNA 607721
204 (biosamples SAMN14144233-SAMN14144256).
205 *Dehydrogenase activity.* This enzymatic activity was determined in greenhouse
206 soil samples with the tetrazolium salt method (Trevors, 1984). The activity was
207 expressed in µg of iodonitrotetrazolium formazan (INTF) g^{-1} dry soil h^{-1}.
208 **Slurry biodegradation experiment.** Accelerated biodegradation assays involved
209 nutrient addition, shaking, monitoring of the biodegradation activity through ^{14}C-
210 mineralization measurements, and single-step chemical analysis of the native PAHs in
211 the residue at the radiorespirometric plateau (i.e., after 55 days). The methodology is
212 described in detail elsewhere (Posada-Baquero et al., 2019a) and briefly in the SI.
213
214 **RESULTS**
215 **Desorption of PAHs.** The desorption kinetics of PAHs present in the creosote-polluted
216 soil at the start of the greenhouse experiment were determined under abiotic conditions
217 by Tenax extraction. Figure 1 shows the results for pyrene and benzo(*a*)pyrene,

representative of mPAHs and cPAHs, respectively, and indicates that the biphasic model allows a good prediction of spontaneous desorption. The theoretical recovery of the fast-desorbing fraction of each chemical after 20 h of extraction with Tenax (D_{20}) was higher than 97%. Considering that, in accordance with this model, slow desorption would still progress well beyond that period, the predicted concentration in soil after 210 days of desorption (the experimental period in the greenhouse experiment) would be expected to decrease from 59.4 mg kg^{-1} to 6.3 mg kg^{-1} for pyrene and from 3.8 mg kg^{-1} to 0.7 mg kg^{-1} for benzo(*a*)pyrene. The results with the other PAHs were also fitted to the biphasic model, and the fit parameter values are shown in Table S1. The kinetic analysis of desorption showed a similar distribution between the fast- and slow-desorbing fractions for all mPAHs. F_{fast} values tended to increasingly decrease with increasing cPAHs molecular weight. The fast-desorbing fraction accounted for 59% and 50% of the total amounts of mPAHs and cPAHs initially present in the creosote-polluted soil, respectively. In accordance with this analysis, we considered D_{20} measurements a good indicator for the evolution of the fast-desorbing fraction with time under the different greenhouse treatments. Eventual shifts in D_{20} values would imply changes in the kinetic fractions and, consequently, in the bioavailability of PAHs.

Greenhouse experiment. *Plant response.* The initial concentration of PAHs in the soil had no significant effects on the plants, either as seed germination percentage, plant development or flowering, as evidenced in preliminary assays with contaminated and agricultural soils. Therefore, sunflower plants tolerated contaminated soils well. The seed germination rate was 48.5% at 44 days from the start of the greenhouse experiment. As the experiment progressed, the plant length reached an average of 63.7 cm at 73 days. By this time, the average number of leaves per plant was 11.6. The flowering period started at 56 days, with 20% of flowered plants, reaching 55% at day

59, and at day 63, all the plants had bloomed. As expected according to the ontogenetic cycle of sunflower in the assayed greenhouse conditions, the plants started to decline at day 70. The addition of rhamnolipid at day 75 sped up this process, causing wilt and strong decay of the plants. In the next few days, plant decay was quite evident in all planted pots.

Dissipation of PAHs and evolution of D_{20}. Total PAH concentrations (Figures 2A, 2C, 3A and 3C) showed a significant decrease after 75 days in planted and unplanted pots, both for mPAHs ($C/C_0 = 0.1$) and cPAHs ($C/C_0 = 0.5$). No significant effect of planting was observed in this initial phase. The concentration of fast-desorbing PAHs (estimated as D_{20}, Figures 2B, 2D, 3B and 3D) also declined during the first 60 days to reach a D_{20} value of approximately 0.1 in all cases. This indicates that biodegradation efficiently removed most of the fast-desorbing chemicals initially present but also part of the slowly desorbing PAHs. As a result, the soil was mainly left with slowly desorbing PAHs. However, a slight increase in D_{20} was observed in planted soils at day 75, parallelling plant decay. Rhamnolipid was therefore added to enhance the bioavailability of the PAHs. This addition had no significant effects on the decline in total PAH concentrations (Figures 2 and 3), which followed similar slow rates in the four treatments with contaminated soil until 210 days. However, a significant ($p \leq 0.05$) increase in the rapidly desorbable fraction was observed shortly after rhamnolipid addition in planted soils for both mPAHs and cPAHs (Figures 2B and 2D, respectively) that did not occur in unplanted soils (Figure 3B and 3D). The increased D_{20} values in the rhamnolipid-amended and planted soils were observed during a period of 45 days, to subsequently decline to reach similar values as in un-amended soils, possibly as a result of biodegradation of the rhamnolipid. Therefore, the biosurfactant made a significant fraction of the slowly desorbing PAHs potentially bioavailable but only when the soil

had supported the growth of plants. This enhancement was, however, not directly translated into accelerated biodegradation under the greenhouse conditions tested.

Dynamics of soil bacterial populations. The bacterial abundance was relatively high at the beginning of the experiment ($5.4 \cdot 10^9$ 16S rRNA gene copies g^{-1} soil) and did not experience significant variations during the period of maximum PAH biodegradation (0-60 days, Figure S1) in either planted or unplanted soil. Bacterial activity, however, seemed to experience a slight increase that was statistically significant only for the planted soil (from $2.2 \cdot 10^9$ to $6.4 \cdot 10^9$ 16S rRNA transcript copies g^{-1}). This increased activity coincided with a reduction in richness and diversity in the active bacterial community (Table S3), also more pronounced in the presence of plants, and with major structural changes (Figures S2 and S3, Table S4). In planted and unplanted soils, specific members of *Pseudomonas* (OTU1; 15.6% and 11.9%, respectively), the actinobacterial genus *Georgenia* (OTU3; 13.1%, 5.3%), and unclassified *Gammaproteobacteria* (OTU6, 3.7%, 8.7%), which had very low frequencies (0.1-0.3%) in the initial soil, became the most active members of the community. The significant increase in the number of transcripts of PAH ring-hydroxylating dehydrogenase (RHD) genes during this period (from $2.4 \cdot 10^6$ to $6.1 \cdot 10^7$ and to $5.2 \cdot 10^7$ gene copies g^{-1} in planted and unplanted soils, respectively) strongly supports that their activity was associated with the removal of the labile fraction of PAHs. In fact, OTU1 presented the highest sequence identity (99%, NCBI-BLAST) with a strain of *Pseudomonas stutzeri*, a species that includes a number of naphthalene- and anthracene- degrading strains; likewise, OTU 6 was closely related to a recently isolated pyrene-degrading strain describing the new order *Immundisolibacterales* (Corteselli et al., 2017). After the first 60 days, with most of the fast-desorbing PAHs removed, the bacterial abundance and activity in the absence of rhamnolipids showed a

293 slow but progressive decline until the end of the experiment in both planted and non
294 planted soils. The decrease in activity resulted in a more even distribution of active
295 microbial phylotypes compared to the distribution in the active microbiome at 60 days,
296 but the previously detected predominant OTUs *Pseudomonas* (OTU1), *Georgenia*
297 (OTU3) and unclassified *Gammaproteobacteria* (OTU 6) were still predominant in both
298 planted and unplanted soils.

299 The addition of rhamnolipid prompted a significant increase in the total bacterial
300 populations of both unplanted ($1.9 \cdot 10^{10}$ gene copies g^{-1}) and planted soil ($6.5 \cdot 10^{10}$ gene
301 copies g^{-1}) at day 135 (Figure S1). In addition, we observed a dramatic shift in the
302 active bacterial community structure (Figures 4, S2, and S3) and a decrease in richness
303 (Table S3), which are both indicative of the selective stimulation of specific
304 components of the community. Those changes were magnified by the presence of
305 plants. The diversity of the active bacterial community decreased as it became
306 predominated by different representatives of *Pseudomonas* (OTU2, OTU5, OTU12),
307 *Comamonadaceae* (OTU4), an unclassified *Enterobacteriacea*e (OTU8) and
308 *Achromobacter* (OTU11), some of which were not detectable in the absence of
309 rhamnolipid. Most of these stimulated bacterial groups best matched (Table S4) strains
310 closely related to plant-associated bacteria characterized by their fast growth and
311 catabolic versatility. For example, OTU11 was classified within the genus
312 *Achromobacter*, which includes opportunistic root colonizers. OTUs 2, 5 and 12 belong
313 to the *Pseudomonas aeruginosa* group, while OTUs 4 and 8 best match rhizospheric or
314 endophytic bacteria, probably those specializing in the utilization of plant-supplied
315 carbon sources. These opportunistic species are also known for their resistance to
316 toxicants in general and specially surfactants. The stimulated microbial community did
317 not seem to have the ability to degrade PAHs, as indicated by the drastic decline in the

318 ratios between copy numbers of RHD genes and 16S rRNA in the presence of
319 rhamnolipid (Figure S4).

320 *Linking biosurfactant action to biodegradation of PAHs.* We investigated why
321 the observed enhancement in D_{20} values in planted soils that received rhamnolipid did
322 not translate, under greenhouse experimental conditions, into decreased residual PAH
323 concentrations. We evaluated two hypotheses that might explain such results: (i) the
324 dissolved soil components (including the biosurfactant) interfere with the performance
325 of the Tenax extraction and (ii) ecophysiological limitations of the biodegradation
326 process, different from the bioavailability limits, eventually occur in the greenhouse
327 conditions. We experimentally tested these hypotheses with greenhouse soil samples
328 taken at day 135, when the bioavailability increase had been sustained in planted soils
329 for 45 days (Figures 2 B and D).

330 (i) For the first hypothesis, the biosurfactant or dissolved SOM present in the
331 aqueous phase could act as a carrier, facilitating the phase exchange of the PAHs from
332 the soil to Tenax, thus increasing D_{20} values. However, the chemical analysis of the
333 aqueous phase of suspensions with the same soil samples, mimicking Tenax extraction
334 conditions, did not reveal any difference among the four treatments in TOC, surface
335 tension, and other relevant parameters such as pH, inorganic carbon, and total nitrogen
336 (Table S2).

337 (ii) Regarding the second hypothesis, increased dehydrogenase activity, an
338 indicator of respiratory activity in PAH-polluted soils (Sushkova et al., 2018, Liu et al.,
339 2018), was found in the cases where rhamnolipids were added (Table 1). This increase
340 occurred particularly in planted soil, where the activity was maximum and double the
341 activity at the beginning of the experiment (1.8 ± 0.2 µg INTF g^{-1} h^{-1}). However, given
342 the general nature of this microbial indicator and the impact of rhamnolipids observed

on different bacterial groups, a biostimulation experiment with increased specificity was designed in soil slurries to test the disappearance of the PAHs under laboratory conditions involving shaking and nutrient addition. These conditions would a priori overcome potential limitations occurring in the greenhouse experiment. Table 1 shows the results of this experiment with pyrene and benzo(*a*)pyrene. Radio-respirometry measurements showed immediate (i.e., without a significant lag phase) production of $^{14}CO_2$ from ^{14}C-labeled pyrene in all treatments (Figure S5). This was expected because of the significant dissipation observed for this chemical under greenhouse conditions. Furthermore, the results indicate that increased D_{20} values were often associated with a significantly increased rate of pyrene mineralization, as evidenced, for example, by the four-fold differences in rates between soil and planted soil amended with rhamnolipid (Table 1). These dissimilar rates confirmed, as expected, that the added ^{14}C-pyrene behaved similarly to the bioavailable fraction of the native compound. The residual concentrations of native pyrene and benzo(*a*)pyrene also declined significantly after slurry-phase treatment in soil samples with relatively high D_{20} values. This result differed from those observed in greenhouse conditions, where the final total concentrations (after 201 days, as indicated by the C_{210d} values in Table 1) did not follow this trend.

DISCUSSION

The results indicate a sustained increase in D_{20} values in planted soil that had received the biosurfactant. This enhanced mobilization potential of the slowly desorbing PAHs is possibly connected to biochemical influences on the rhamnolipid sorbed onto soil aggregates. The biosurfactant partitioned in the aqueous phase might act as a carrier by facilitating the phase exchange of the PAHs from the soil to the Tenax, thus

368 increasing D_{20} values. This role would be similar to that already observed for DOC in
369 bioavailability assessments of PAHs with cyclodextrin-assisted depletive extraction
370 (Bartolome et al., 2018) and passive sampling (Haftka et al., 2008). However, the
371 complete absence of differences in TOC and surface tension in the aqueous solutions
372 from Tenax extractions of soil treatments giving dissimilar D_{20} values excludes this
373 possibility. We can conclude, therefore, that the enhanced desorption rate, resulting in
374 increased D_{20} values, was an effect of the biosurfactant present in the soil aggregates but
375 only if the soil had supported the growth of plants.

376 The plant-promoted growth of specific bacterial species and the increased soil
377 respiratory potential observed after rhamnolipid addition to planted soil suggest a
378 microbial cause for this enhancement in D_{20} values. The promotion of specific groups of
379 bacteria by rhamnolipid could be explained by the capability of the biosurfactant to
380 generate a new flux of carbon to bacterial cells by directly serving as a source of carbon
381 and energy or by indirectly mobilizing easily degradable organic matter present in the
382 soil, thus favoring the development of fast-growing bacterial groups (Shao et al., 2017).
383 In the presence of plants, this effect would have been magnified since rhamnolipid
384 accelerated the plant decay, making easily degradable organic matter of plant origin
385 available to bacterial populations specialized in their utilization. This mechanism is
386 compatible with the similar TOC values detected in the aqueous phase of soil
387 suspensions from all treatments after 135 days if the proliferation of the stimulated soil
388 microorganisms had already been completed. In addition to having this nutritional
389 impact on the soil microbial community, rhamnolipids may have favored the growth of
390 certain bacterial groups by increasing membrane permeation and exoenzyme secretion,
391 but they may have also inhibited the growth of others by disrupting the functioning of
392 their cell membrane (Shao et al., 2017).

Provided that the primary mechanism underlying the rhamnolipid association with the soil is an adsorption process at the soil-water interface (Congiu and Ortega-Calvo, 2014), it is possible that the stimulated microbial components of the soil aggregates contributed to such an enhancement in D_{20} values if the new microbial biomass produced and possibly its associated exopolysaccharides interacted with rhamnolipids to enhance their penetration into the soil aggregates. This would have resulted in swelling of the sorbent, favoring the intra-aggregate diffusion of PAHs by this biomass acting as an alternative partitioning phase (Garcia-Junco et al., 2003, Mulder et al., 1998) and ultimately enhancing the kinetics of desorption of the chemicals. Alternately, it is also possible that root components released into the soil, such as fatty acids (Yi and Crowley, 2007), interacted with rhamnolipids to enhance PAH diffusion. Whether the increased efficiency of the biosurfactant was indirectly caused by the growth of specific bacteria, directly caused by plant components, or both should be the subject of further investigation. In any case, although the increased D_{20} values did not result in significant reductions of PAH residual concentrations in the greenhouse experiments, the bioavailability enhancements were evidenced in slurry experiments as increased mineralization rates and decreased residual PAH concentrations. This biostimulation overcomes other possible limitations to the biodegradation process that eventually occur in greenhouse conditions and thus leads, for example, to the PAH degraders being outcompeted by the bacterial groups favored by rhamnolipid addition. These results have two main implications for the bioremediation of PAH-polluted soils. On the one hand, they suggest that, with appropriate process optimization, the observed bioavailability enhancement can be translated into improved bioremediation. On the other hand, if such optimization is not performed, such an increased bioavailability may result in increased exposure to the mobilized pollutants by potential human or

418 ecological targets. The latter implications align with recent considerations of the
419 potential risks caused at the initial stages of bioremediation as a result of unmodulated
420 biological processing of the pollutants that leads to the eventual formation of
421 byproducts that are more toxic than the parent PAHs (Rolando et al., 2020).

422 Our study extends the limited knowledge of the mechanisms responsible for
423 increasing biosurfactant action on slowly desorbing PAHs, which limits the competitive
424 use of this method in bioremediation as a sustainable alternative to chemical surfactant
425 application. The proposed sequential approach based on plant development followed by
426 biosurfactant application fits well in low-risk soil remediation approaches that are
427 oriented towards the application of phase-exchange promoters, once the fast desorbing
428 PAHs are removed through conventional bioremediation (Ortega-Calvo et al., 2013,
429 Bueno-Montes et al., 2011, Posada-Baquero et al., 2019a, Adrion et al., 2016). Our
430 results show that the rhizosphere-enhanced biosurfactant action exceeds the
431 solubilisation potential already observed in the studies regarding the solubilisation of
432 slowly desorbing PAHs. Taking benzo(a)pyrene as a representative cPAH, we observed
433 that 45% of the compound was made bioavailable in planted soil that received the
434 biosurfactant (D_{20} = 0.45, Table 1). This is a significant mobilization potential
435 considering that, for example, rhamnolipid alone can mobilize only 18% of the
436 compound in a bioremediated soil from a manufactured gas plant site (at a concentration
437 ten times higher than in this study, 70 mg g^{-1}, and after 312 h of continuous extraction)
438 (Posada-Baquero et al., 2019a).

439 The new sequential approach proposed in this study, based on the relatively
440 short ontogenetic cycle of sunflower, would not only decrease decontamination
441 endpoints through the improved biosurfactant action described above but also avoid
442 possible toxic effects caused by the rhamnolipid and solubilized pollutants on plant

development when the biosurfactant is applied at the start of the process. Indeed, 4 mg kg^{-1} rhamnolipid, a similar concentration to that used in our study, causes growth reduction in sunflower development in hydrocarbon-contaminated soil (Liduino et al., 2018). Similarly, phytotoxicity has been reported for the chemical surfactants Brij35 and Tween 80 in the phytoremediation of soils with ryegrass plants and red clover, respectively (Gao et al., 2006, Gao et al., 2008). The negative effects of chemical and biological surfactants can also affect the microbial soil populations in terms of the toxicity and competition effects between mPAHs and cPAHs when the surfactants are applied to soils with a relatively high fraction of fast-desorbing PAHs but not to those having mainly slowly desorbing PAHs (Bueno-Montes et al., 2011, Posada-Baquero et al., 2019a).

CONCLUSIONS

By an adequately integrating of the sunflower ontogenetic cycle into the bioremediation of PAH-polluted soils, we have demonstrated that it is possible to enhance the limited biosurfactant efficiency that is commonly observed under unfavorable conditions in contaminated field soils. The residual, slowly-desorbing PAHs that remain after the initial phase of fast biodegradation were mobilized significantly by the rhamnolipid added at this late stage but only if the soil had supported the growth of plants. This effect can likely be attributed to a rhizosphere influence on biosurfactant action. These results have relevance not only in the bioremediation field but also in the risk assessment and management of organic chemicals in general, where bioavailability is under discussion. This new, proof-of-concept scenario successfully showed the use of desorption extraction as a reliable approach to investigate changes in bioavailability under widely ranging operating conditions that include different time scales and dissimilar treatments involving biosurfactant application.

ASSOCIATED CONTENT

Supporting Information

Additional information on materials and methods, and tables and figures showing desorption kinetics of individual PAHs, chemical analysis of the aqueous phase in Tenax extractions, taxonomic classification and relative abundance of OTUs in soils, dynamics of soil bacterial populations, evolution of ring-hydroxylating dioxygenase genes, and radiorespirometry results with ^{14}C-pyrene.

AUTHOR INFORMATION

Corresponding Author

*Phone: (+34) 954 624 711; Fax: (+34) 954 624 002;

E-mail: jjortega@irnase.csic.es.

Notes

The authors declare no competing financial interest.

ACKNOWLEDGMENTS

We thank the Spanish Ministry of Economy, Industry and Competitiveness (CGL2016-77497-R), and the Andalusian Government (RNM 2337). Joaquim Vila is a Serra Húnter Fellow (Generalitat de Catalunya). Sara N. Jiménez-Volkerink is recipient of a pre-doctoral fellowship from the Spanish Ministry of Science, Innovation and Universities (FPU15/06077).

REFERENCES

ADRION, A. C., NAKAMURA, J., SHEA, D. & AITKEN, M. D. 2016. Screening nonionic surfactants for enhanced biodegradation of polycyclic aromatic hydrocarbons remaining in soil after conventional biological treatment. *Environmental Science and Technology,* 50**,** 3838-3845.

BARTOLOME, N., HILBER, I., SOSA, D., SCHULIN, R., MAYER, P. & BUCHELI, T. D. 2018. Applying no-depletion equilibrium sampling and full-depletion bioaccessibility extraction to 35 historically polycyclic aromatic hydrocarbon contaminated soils. *Chemosphere*, 199**,** 409-416.

BUENO-MONTES, M., SPRINGAEL, D. & ORTEGA-CALVO, J. J. 2011. Effect of a non-ionic surfactant on biodegradation of slowly desorbing PAHs in contaminated soils. *Environmental Science and Technology,* 45**,** 3019-3026.

CÉBRON, A., NORINI, M.-P., BEGUIRISTAIN, T. & LEYVAL, C. 2008. Real-Time PCR quantification of PAH-ring hydroxylating dioxygenase (PAH-RHDalpha) genes from Gram positive and Gram negative bacteria in soil and sediment samples. *Journal of Microbiological Methods,* 73**,** 148–159.

CONGIU, E. & ORTEGA-CALVO, J.-J. 2014. Role of desorption kinetics in the rhamnolipid-enhanced biodegradation of polycyclic aromatic hydrocarbons. *Environmental Science and Technology,* 48**,** 10869-10877.

CORTESELLI, E. M., AITKEN, M. D. & SINGLETON, D. R. 2017. Description of *Immundisolibacter cernigliae* gen. nov., sp. nov., a high-molecular-weight polycyclic aromatic hydrocarbon-degrading bacterium within the class *Gammaproteobacteria*, and proposal of *Immundisolibacterales* ord. nov. and *Immundisolibacteraceae* fam. nov. *International Journal of Systematic and Evolutionary Microbiology,* 67**,** 925-931.

CHENG, W., PARTON, W. J., GONZALEZ-MELER, M. A., PHILLIPS, R., ASAO, S., MCNICKLE, G. G., BRZOSTEK, E. & JASTROW, J. D. 2014. Synthesis and modeling perspectives of rhizosphere priming. *New Phytologist,* 201**,** 31-44.

GAO, Y., LING, W. & WONG, M. H. 2006. Plant-accelerated dissipation of phenanthrene and pyrene from water in the presence of a nonionic-surfactant. *Chemosphere,* 63**,** 1560-1567.

GAO, Y., SHEN, Q., LING, W. & REN, L. 2008. Uptake of polycyclic aromatic hydrocarbons by Trifolium pretense L. from water in the presence of a nonionic surfactant. *Chemosphere,* 72**,** 636-643.

GARCIA-JUNCO, M., GOMEZ-LAHOZ, C., NIQUI-ARROYO, J. L. & ORTEGA-CALVO, J. J. 2003. Biodegradation- and biosurfactant-enhanced partitioning of polycyclic aromatic hydrocarbons from nonaqueous-phase liquids. *Environmental Science and Technology,* 37**,** 2988-2996.

HAFTKA, J. J. H., PARSONS, J. R., GOVERS, H. A. J. & ORTEGA-CALVO, J. J. 2008. Enhanced kinetics of solid-phase microextraction and biodegradation of polycyclic aromatic hydrocarbons in the presence of dissolved organic matter. *Environmental Toxicology and Chemistry,* 27**,** 1526-1532.

ISO/TS16751 2018. Soil Quality - Environmental availability of non-polar organic compounds- Determination of the potential bioavailable fraction using a strong adsorbent or complexing agent. International Organization for Standardization: Geneva, Switzerland.

KOZICH, J. J., WESTCOT, T. S. L., BAXTER, N. T., HIGHLANDER, S. K. & SCHLOSS, P. D. 2013. Development of a dual-index sequencing strategy and curation pipeline for analyzing amplicon sequence data on the MiSeq Illumina sequencing platform. *Applied and Environmental Microbiology,* 79**,** 5112-20.

LIAO, C., LIANG, X., LU, G., THAI, T., XU, W. & DANG, Z. 2015. Effect of surfactant amendment to PAHs-contaminated soil for phytoremediation by maize (*Zea mays* L). *Ecotoxicology and Environmental Safety,* 112**,** 1-6.

LIAO, C., XU, W., LU, G., DENG, F., LIANG, X., GUO, C. & DANG, Z. 2016. Biosurfactant-enhanced phytoremediation of soils contaminated by crude oil using maize (*Zea mays*. L). *Ecological Engineering,* 92**,** 10-17.

LIDUINO, V. S., SERVULO, E. F. C. & OLIVEIRA, F. J. S. 2018. Biosurfactant-assisted phytoremediation of multi-contaminated industrial soil using sunflower (*Helianthus annuus* L.). *Journal of Environmental Science and Health Part a-Toxic/Hazardous Substances and Environmental Engineering,* 53**,** 609-616.

LIU, X. Y., HU, X. X., ZHANG, X. Y., CHEN, X. P., CHEN, J. & YUAN, X. Y. 2018. Effect of *Bacillus subtilis* and NTA-APG on pyrene dissipation in phytoremediation of nickel co-contaminated wetlands by *Scirpus triqueter*. *Ecotoxicology and Environmental Safety,* 154**,** 69-74.

MULDER, H., BREURE, A. M., VAN HONSCHOOTEN, D., GROTENHUIS, J. T. C. & VAN ANDEL, J. G. 1998. Effect of biofilm formation by *Pseudomonas* 8909N on the bioavailability of solid naphthalene. *Applied Microbiology and Biotechnology,* 50**,** 277-283.

ORTEGA-CALVO, J. J., HARMSEN, J., PARSONS, J. R., SEMPLE, K. T., AITKEN, M. D., AJAO, C., EADSFORTH, C., GALAY-BURGOS, M., NAIDU, R., OLIVER, R., PEIJNENBURG, W., ROMBKE, J., STRECK, G. & VERSONNEN, B. 2015. From bioavailability science to regulation of organic chemicals. *Environmental Science and Technology,* 49**,** 10255-10264.

ORTEGA-CALVO, J. J., TEJEDA-AGREDANO, M. C., JIMENEZ-SANCHEZ, C., CONGIU, E., SUNGTHONG, R., NIQUI-ARROYO, J. L. & CANTOS, M.

2013. Is it possible to increase bioavailability but not environmental risk of PAHs in bioremediation? *Journal of Hazardous Materials,* 261**,** 733– 745

PARKS, D. H., TYSON, G. W., HUGENHOLTZ, P. & BEIKO, R. G. 2014. STAMP: statistical analysis of taxonomic and functional profiles. *Bioinformatics,* 30**,** 3123–3124.

POSADA-BAQUERO, R., GRIFOLL, M. & ORTEGA-CALVO, J.-J. 2019a. Rhamnolipid-enhanced solubilization and biodegradation of PAHs in soils after conventional bioremediation. *Science of the Total Environment,* 668**,** 790-796.

POSADA-BAQUERO, R., LOPEZ-MARTIN, M. & ORTEGA-CALVO, J.-J. 2019b. Implementing standardized desorption extraction into bioavailability-oriented bioremediation of PAH-polluted soils. *Science of the Total Environment,* 696**,** 134011.

POSADA-BAQUERO, R. & ORTEGA-CALVO, J. J. 2011. Recalcitrance of polycyclic aromatic hydrocarbons in soil contributes to background pollution. *Environmental Pollution,* 159**,** 3692-3699.

ROLANDO, L., VILA, J., BAQUERO, R. P., CASTILLA-ALCANTARA, J. C., BARRA CARACCIOLO, A. & ORTEGA-CALVO, J.-J. 2020. Impact of bacterial motility on biosorption and cometabolism of pyrene in a porous medium. *Science of The Total Environment,* 717**,** 137210.

RONDANINI, D. P., SAVIN, R. & HALL, A. J. 2007. Estimation of physiological maturity in sunflower as a function/of fruit water concentration. *European Journal of Agronomy,* 26**,** 295-309.

SHAHBAZ, M., KUMAR, A., KUZYAKOV, Y., BORJESSON, G. & BLAGODATSKAYA, E. 2018. Priming effects induced by glucose and

592 decaying plant residues on SOM decomposition: A three-source C-13/C-14
593 partitioning study. *Soil Biology and Biochemistry,* 121**,** 138-146.
594 SHAO, B., LIU, Z., ZHONG, H., ZENG, G., LIU, G., YU, M., LIU, Y., YANG, X., LI,
595 Z., FANG, Z., ZHANG, J. & ZHAO, C. 2017. Effects of rhamnolipids on
596 microorganism characteristics and applications in composting: A review.
597 *Microbiological Research,* 200**,** 33-44.
598 SIVARAM, A. K., LOGESHWARAN, P., LOCKINGTON, R., NAIDU, R. &
599 MALLAVARAPU, M. 2018. Impact of plant photosystems in the remediation
600 of benzo(*a*)pyrene and pyrene spiked soils. *Chemosphere,* 193**,** 625-634.
601 SUSHKOVA, S. N., MINKINA, T., DERYABKINA, I., MANDZHIEVA, S.,
602 ZAMULINA, I., BAUER, T., VASILYEVA, G., ANTONENKO, E. &
603 RAJPUT, V. 2018. Influence of PAH contamination on soil ecological status.
604 *Journal of Soils and Sediments,* 18**,** 2368-2378.
605 TEJEDA-AGREDANO, M. C., GALLEGO, S., VILA, J., GRIFOLL, M., ORTEGA-
606 CALVO, J. J. & CANTOS, M. 2013. Influence of sunflower rhizosphere on the
607 biodegradation of PAHs in soil. *Soil Biology and Biochemistry,* 57**,** 830-840.
608 TREVORS, J. T. 1984. Dehydrogenase activity in soil: a comparison between the INT
609 and TTC assay. *Soil Biology and Biochemistry,* 16**,** 673-674.
610 YI, H. & CROWLEY, D. E. 2007. Biostimulation of PAH degradation with plants
611 containing high concentrations of linoleic acid. *Environmental Science and*
612 *Technology,* 41**,** 4382-4388.
613 ZHU, B., GUTKNECHT, J. L. M., HERMAN, D. J., KECK, D. C., FIRESTONE, M.
614 K. & CHENG, W. 2014. Rhizosphere priming effects on soil carbon and
615 nitrogen mineralization. *Soil Biology & Biochemistry,* 76**,** 183-192.
616

Figure legends

Figure 1. Kinetics of desorption of pyrene and benzo(*a*)pyrene from a polluted soil determined by Tenax extraction,. The dashed lines represent the results of fitting equation 1 to the desorption data. The percentages denote the theoretical recovery of the fast-desorbing fraction of each chemical after 20 h of extraction with Tenax.

Figure 2. Effect of rhamnolipid addition (indicated by the arrows) on the total (as C/C_0, panels A and C) and rapidly desorbable (as D_{20}, panels B and D) concentrations of mineralizable (A) and cometabolizable (C) polycyclic aromatic hydrocarbons (mPAHs and cPAHs, respectively, as defined in the text) in contaminated soil planted with sunflower and incubated under greenhouse conditions. The circles correspond to the soil after ir received the biosurfactant, whereas the control (squares) did not receive it. The asterisks indicate significant differences (*t*-test, $P = 0.05$) in D_{20} values between the biosurfactant-amended treatments and their respective values at the same sampling time in planted soil receiving no biosurfactant.

Figure 3. The same effects as in Figure 2 but with unplanted soil. The asterisk in panel B indicates significant differences (*t*-test, $P = 0.05$) in D_{20} values between the biosurfactant-amended treatments and the respective values at the same sampling time in unplanted soil receiving no biosurfactant.

Figure 4. Effect of rhamnolipid addition (R) on the active bacterial community structure in planted (black bars) and unplanted soil (white bars) after 135 days of incubation. Only OTUs with an abundance higher than 2.5% are represented. The

642 taxonomic classification of OTUs is based on the RDP database, with an assignation
643 probability >80%. Significant differences (P = 0.05) in the relative abundance of each
644 OTU in the four different conditions are represented with different letters (a/b/c).
645
646

647 **Figure 1**

648

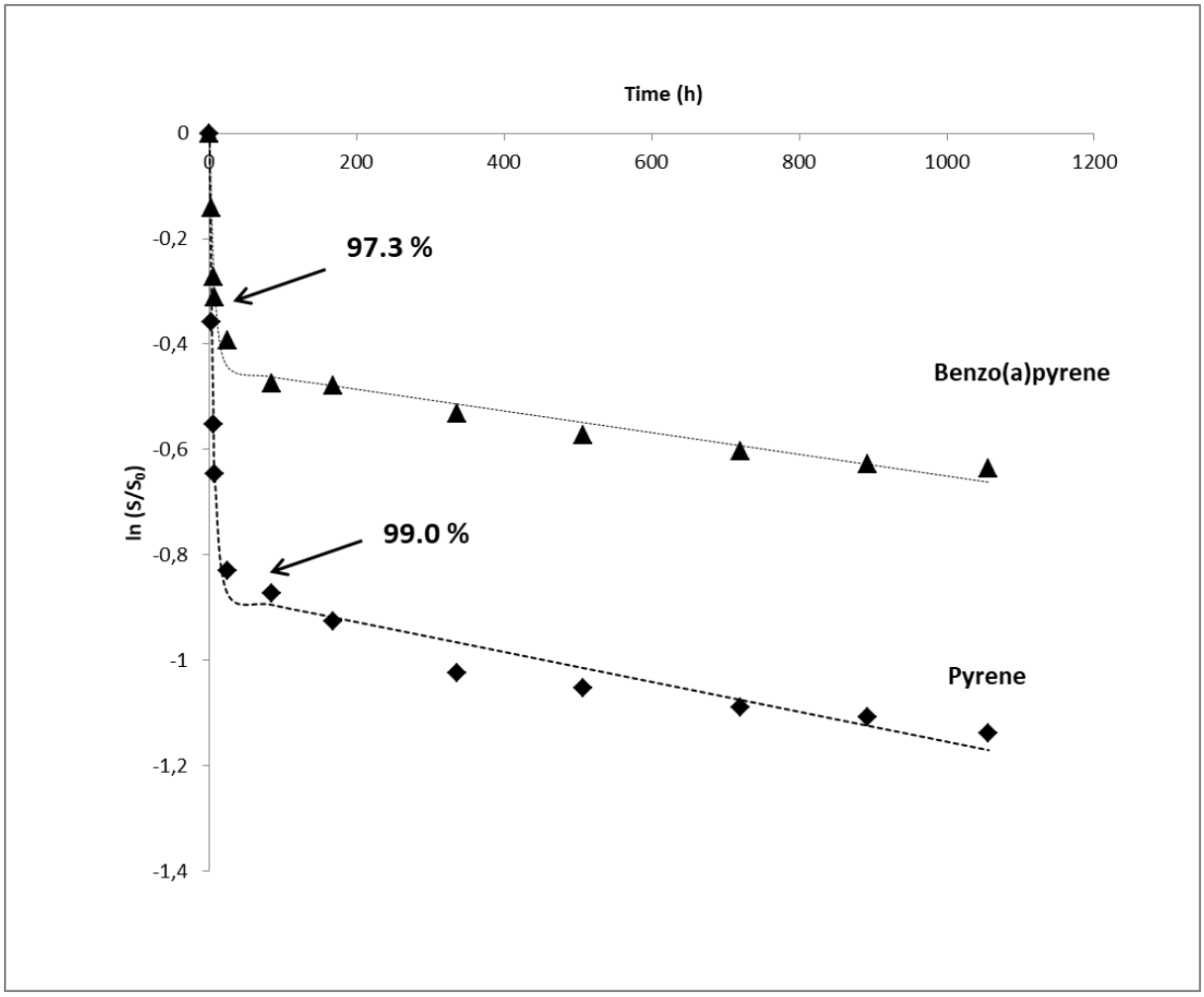

649

650 **Figure 2**

651

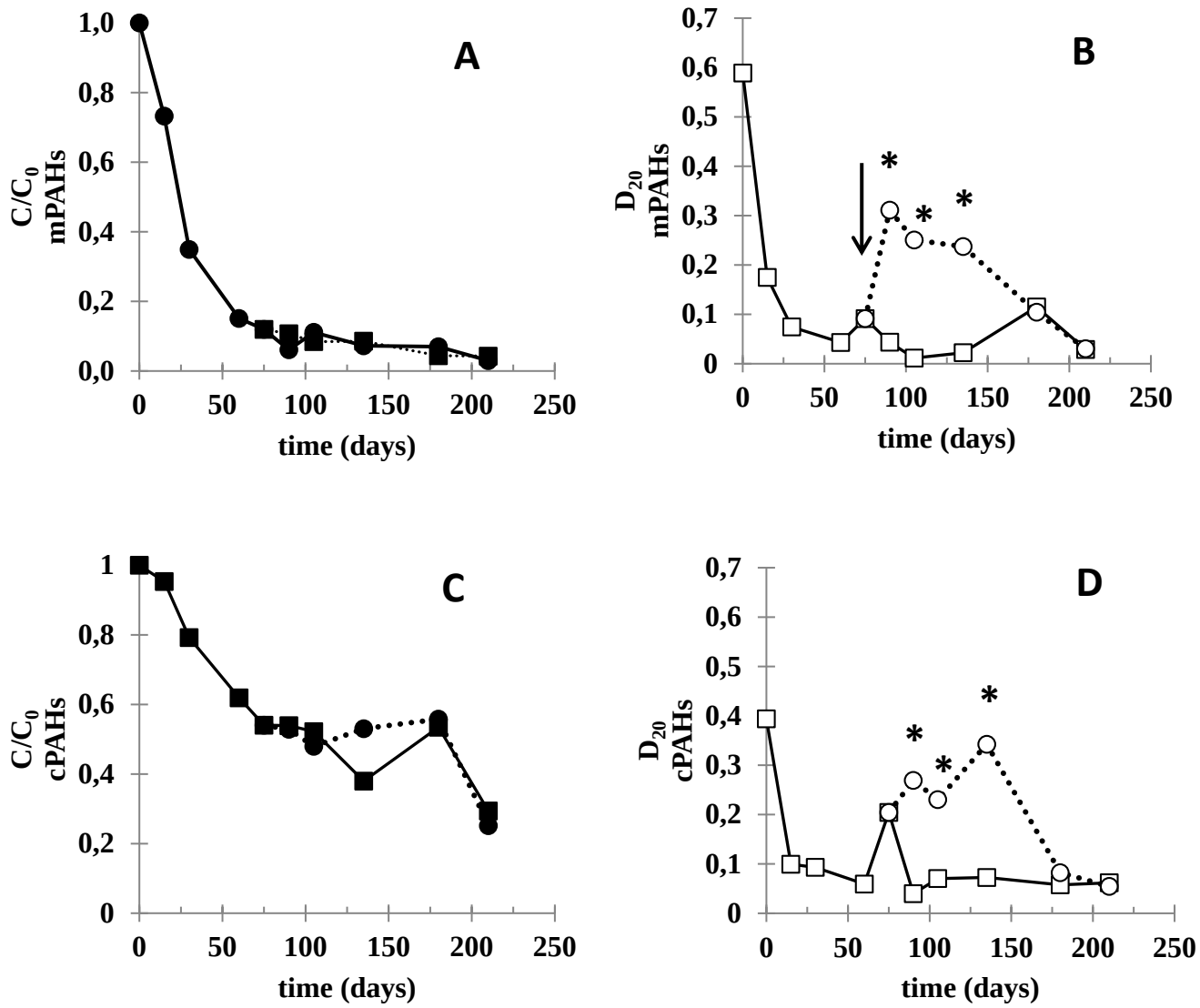

652 **Figure 3**

653

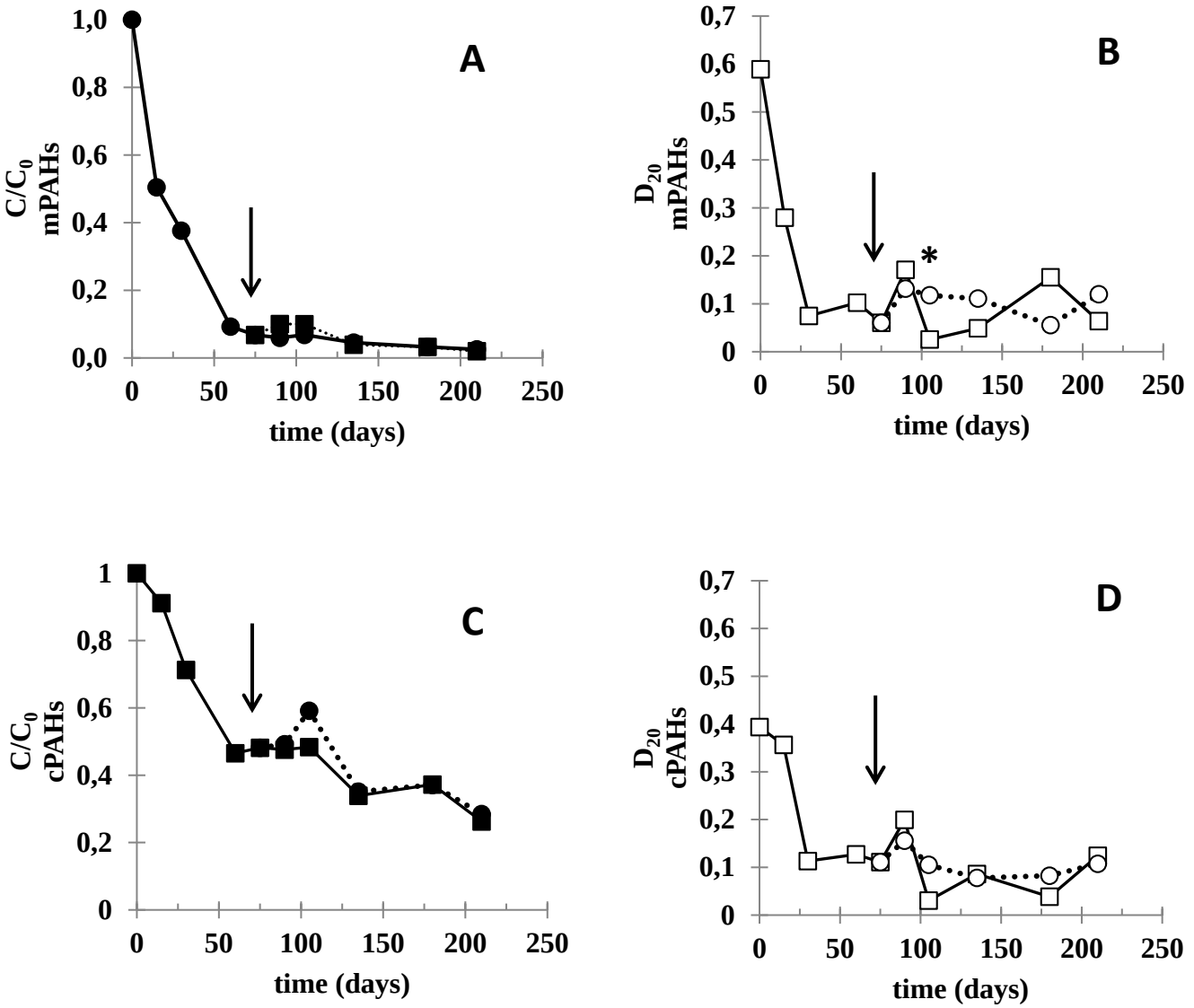

654 **Figure 4**

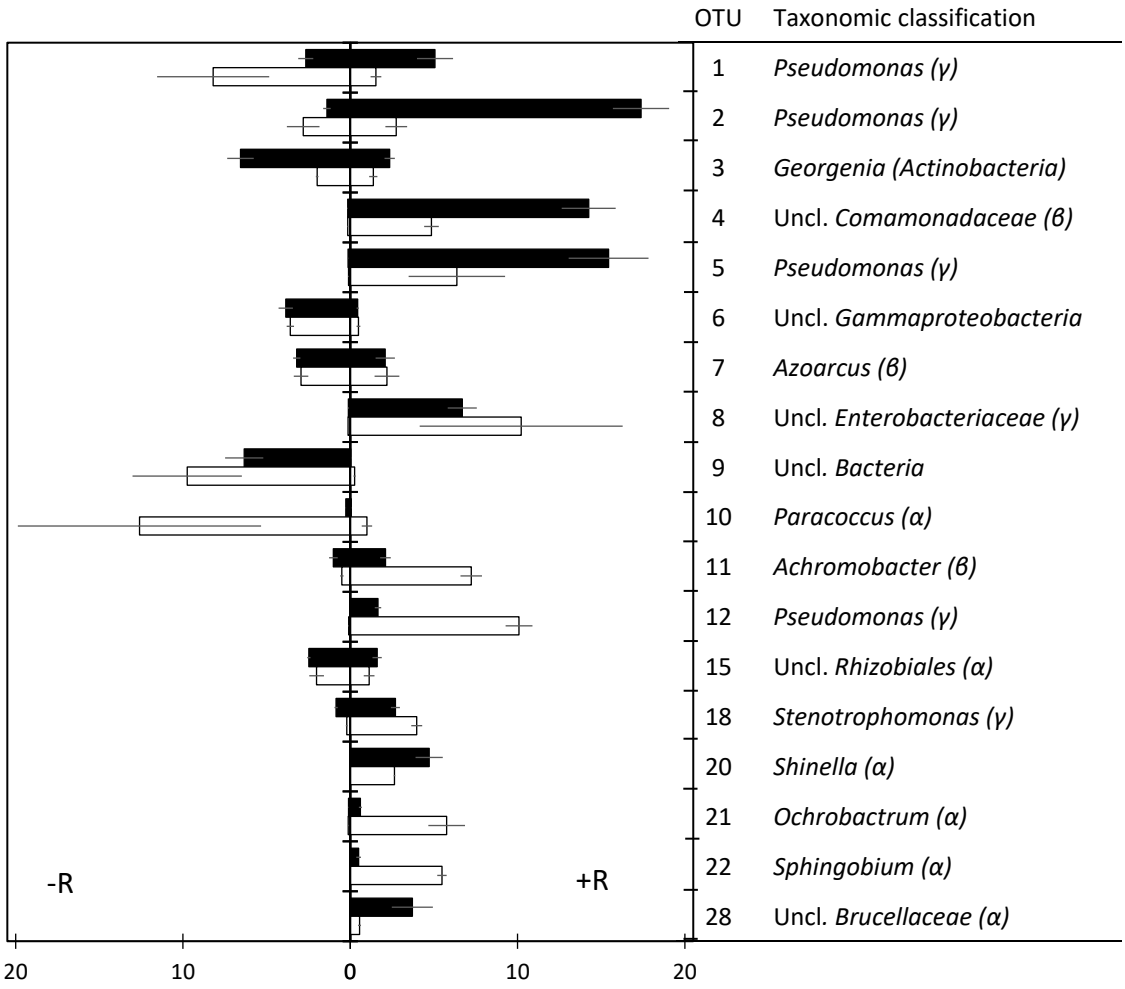

655

Table 1. Dehydrogenase activity (DH) and biodegradability of pyrene and benzo(*a*)pyrene in soil slurries with samples from the greenhouse experiment taken after 135 days.

	Soil	**Soil + rhamnolipid**	**Planted soil**	**Planted soil + rhamnolipid**
DH ($\mu g\ INTF\ g^{-1}\ h^{-1}$)	0.4 ± 0.1a	1.6 ± 0.7b	0.2 ± 0.1a	3.2 ± 1.2c
Biodegradability				
		Pyrene		
D_{20} [a]	0.04	0.13	0.10	0.20
Min. rate ($\mu g\ kg^{-1}\ h^{-1}$)[b]	1.5 ± 0.1a[d]	1.7 ± 0.2ab	3.9 ± 0.9bc	5.3 ± 0.01c
Min. extent (%)[b]	40 ± 6	38 ± 8	48 ± 6	40 ± 7
C_0 ($mg\ kg^{-1}$)[b]	4.0 ± 0.2A[e]	6.3 ± 0.3A	5.0 ± 1.0A	13.8 ± 4.4 A
C_f ($mg\ kg^{-1}$)[b]	1.0 ± 0.1Aa	0.5 ± 0.1Bab	0.6 ± 0.2Bab	0.4 ± 0.01Bb
C_{210d} ($mg\ kg^{-1}$)[c]	2.8 ± 0.8A	2.4 ± 0.2AB	3.7 ± 0.4A	2.7 ± 0.2AB
		Benzo(*a*)pyrene		
D_{20} [a]	0.10	0.10	0.18	0.45
C_0 ($mg\ kg^{-1}$)[b]	1.9 ± 0.5A	1.6 ± 0.01A	1.8 ± 0.15A	2.5 ± 0.5A
C_f ($mg\ kg^{-1}$)[b]	0.8 ± 0.1Aa	0.6 ± 0.04Bab	0.7 ± 0.05Aab	0.5 ± 0.01Bb
C_{210d} ($mg\ kg^{-1}$)[c]	1.6 ± 0.2A	1.8 ± 0.01A	1.5 ± 0.5A	1.6 ± 0.04AB

[a] D_{20}: rapidly desorbable fraction of pyrene or benzo(*a*)pyrene extracted with Tenax (20 h). [b] Min. rate, min. extent, C_0 and C_f: rate and extent of pyrene mineralization and initial and final concentrations of pyrene or benzo(a)pyrene in slurry experiments over 55 days, respectively. [c] C_{210d}: concentrations of pyrene or benzo(a)pyrene in soils from greenhouse experiments after 210 days. [d] Values in rows with the same lowercase letter are not significantly different (ANOVA, $P = 0.05$).[e] Values for each compound in columns with the same capital letter are not significantly different (ANOVA, $P = 0.05$).